A CASE STUDY OF EXTREM ASPECT SENSITIVE VHF RADAR BACKSCATTER IN THE VICINITY OF PMSE DURING THE ECOMA 2008 ROCKET CAMPAIGN

Norbert Engler, Werner Singer, Ralph Latteck, Markus Rapp, and Boris Strelnikov

Leibniz Institute of Atmospheric Physics at Univ. of Rostock
Schlossstr. 6, D-18225 Kühlungsborn

ABSTRACT

Radar measurements with a high temporal and vertical resolution were conducted at Andenes, North Norway, during the ECOMA rocket campaign in 2008. The results obtained from these measurements show a distinct double layer structure of PMSE for the period of the ECOMA-04 rocket flight at altitudes between 80 and 90 km. The structure of these radar echoes at 50 MHz are investigated in more detail, including the aspect sensitivity, turbulence, and the simultaneously measured background wind field. It turns out that the radar echoes during this rocket flight are highly aspect sensitive with different aspect ratios across the observed altitude range. The in-situ turbulence observation using rocket-borne instruments allows a more detailed discussion of the fine structure observed in the radar sounding. The results indicate strong anisotropic scattering structures, especially at bounderies between strong turbulent and less turbulent altitudes.

Key words: Radar backscatter, aspect sensitivity, turbulence, ECOMA.

1. INTRODUCTION

During the summer period radar backscatter at a frequency of around 50 MHz shows very strong echoes from mesospheric altitudes, especially at polar latitudes. These echoes are known as polar mesosphere summer echoes (PMSE) and have been observed for more than 20 years [1, 2, 3, 4]. A recent review [4] summarizes the observations and the current understanding of these echoes. The strong echoes originate from inhomgeinities in the electron density due to the existence of charged ice particles which reduce the mobility of free electrons. Turbulence and the reduced mobility of the electrons are the driving forces which create structures with a vertical extent in the order of the Bragg scale (half of the radar wavelength) which is significantly smaller than the inner scale of neutral air turbulence. Owing to their superior signal to noise ratio, PMSE are well suited to observe the thermal and dynamical state of the mesopause region and provide access to important atmospheric parameters like neutral air turbulence, winds, gravity wave parameters, and long term changes.

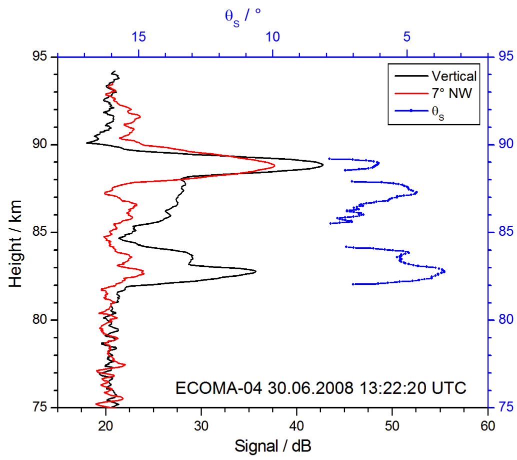

Figure 1. Signal strength of the vertical and off-zenith pointing beams (bottom axis) and the aspect sensitivity parameter θ_s (top axis, reversed). A small value of θ_s corresponds to a high aspect sensitivity with larger anisotropic structures and a high θ_s to low and less anisotropic backscattering structures. The median height profiles were averaged for 15 min around the launch time.

The ALWIN MST radar [5] is located near the Andøya Rocketrange (69°N, 16°E) and is operating with a frequency of 53.5 MHz which is well suited for the observation of PMSE near the polar summer mesopause since PMSE are observed with nearly 100% occurrence rate at this frequency. It allows the study of the dynamical state at mesospheric altitudes. In June/July 2008 an extensive campaign in the frame of the ECOMA project was conducted with rocket-borne and ground-based instruments. An overview about the acitivties and the scientific goals of the ECOMA project is given in [6]. During this campaign VHF radar measurements were conducted with a high temporal and vertical resolution to observe physical parameters of the strong echoes from ground. Around the period of the rocket launch a special program with high temporal and vertical resolution was used provid-

Proc. '19th ESA Symposium on European Rocket and Balloon Programmes and Related Research, Bad Reichenhall, Germany, 7–11 June 2009 (ESA SP-671, September 2009)

ing a vertical and north-westwards pointing beams with off-zenith angles of 7° and 14°. A pulse of 2 µs was transmitted corresponding to a range resolution of 300 m. The backscattered signal was sampled with 50 m resolution. In this experiment an interpulse period of 800 µs was applied. The parameters of this experiment allow a maximum detectable radial velocity of 27.36 m/s. In the case study presented here results obtained from the vertical and the 7° off-zenith beam were selected to discuss the interesting phenomena of aspect sensitive radar backscatter in the vicinity of PMSE.

The radar observation shows a distinct double-layer structure during the ECOMA-04 rocket launch. The results show a strong dependence of the signal strength on the tilt angle. This angular dependence can be described by the aspect sensitivity parameter [7, 8] and can be used to gain information about the anisotropy of the scatterers. From modeling studies of shear structures [9] and the perturbations due to horizontally propagating interia-gravity waves [10, 11] it is known that the turbulent velocity field generated by such processes is often anisotropic. The background of the modelling studies is used to analyze the radar observations concerning the shape of the scatterers in terms of turbulent cells. The special case observed during the ECOMA-04 rocket flight is discussed in more detail in the following sections. The combination of radar measurements of aspect sensitivity together with the in-situ results of turbulent motion is used to explain the high aspect sensitivity observed during this particular rocket launch.

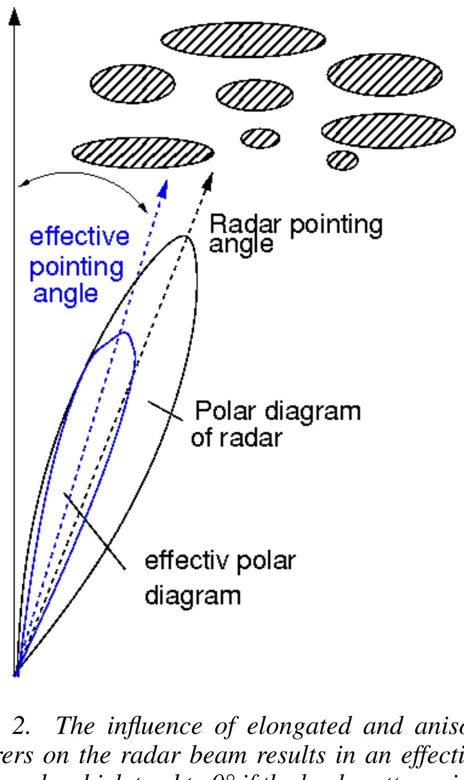

Figure 2. The influence of elongated and anisotropic scatterers on the radar beam results in an effective off-zenith angle which tend to 0° if the backscatter originates from mirror-like reflectors. The radar beam is altered due to the asymmetry introduced by the scatterers. (draw after [12]

2. DETERMINING THE ASPECT SENSITIVITY PARAMETER θ_S

It has been known for many years that PMSE are highly aspect sensitive [7, 8, 13] which means that the backscattered power is a function of the pointing direction of the radar beam. In the common parameterization the scatterers at a given height can be expressed by a backscatter polar diagram in the form of $\exp\left(-\theta^2/\theta_s^2\right)$ describing the mean backscattered power expected with the scatterer positioned at an angle θ from the zenith. The form of a radar beam looking vertically is given by $\exp\left(-\theta^2/\theta_0^2\right)$. Using a radar beam tilted for θ_t off-zenith, the highest field strength is received at an effective pointing angle $\theta_{eff} = \theta_t/R_1$, with $R_1 \approx 1 + \theta_0/\theta_s$ [8]. These expressions imply that the polar diagrams of the radar beam and the scatterer itself have a Gaussian distribution with a certain width (θ_0, θ_s, respectively). The parameter θ_s describes the degree of aspect sensitivity for a height bin. Whilst θ_s approaches 0° the echo would result from a mirror-like reflector but approaching infinity would result in an isotropic scatterer. In practice at a value of $\theta_s \approx 20°$ the scatterer can be regarded as almost isotropic [13]. Fig. 2 shows schematicly the influence of elongated structures on a tilted Doppler beam. The magnitude of the signals varies with the tilt angle with strongest echoes from overhead. This effect is a result of the anisotropic nature of the scatterers and effects the horizontal and vertical wind measurements because the mean backscatter is received from structures with an effective pointing angle. Relating the polar diagrams of the vertical and an off-zenith pointing radar beam to each other the received echo power is given as [8, 13]

$$\frac{P(\theta_T)}{P(0°)} = \exp\left[-\left(\frac{(\theta_{eff}-\theta_t)^2}{\theta_0^2} + \frac{\theta_{eff}^2}{\theta_s^2}\right)\right]\frac{h^4}{r_t^4} \qquad (1)$$

h and r_t are the height of the scattering layer and the range to scattering layer in the off-zenith direction, respectively. The term h^4/r_t^4 differs not much from unity with respect to the other terms and can be neglected for pointing angles less than 10° [13]. Using θ_{eff} and turning around Eq. 1 the aspect sensitivity parameter θ_s can be calculated after

$$\sin^2\theta_s = \frac{\sin^2\theta_T}{\ln\left(\frac{P(0)}{P(\theta_T)}\right)} - \sin^2\left(\frac{\theta_0^{(2w)}}{\sqrt{\ln 2}}\right) \qquad (2)$$

as given in [13, 14] where the two-way 1/e-width of the radar beam $\theta_0^{(2w)}$ is used for the determination of the aspect angle.

We apply the model in [15] which assumes that the refractive index of an individual scatterer varies horizontally with a Gaussian shape and vertically in an equally smooth manner. The structure is assumed to have an ellipsoidal shape in the vertical plane and a circular symmetry in the horizontal plane. Furthermore, it is assumed that all scatterers have the same aspect ratio l_x/l_z which represent an average shape produced by anisotropic turbulence. Considering ellipsoidal scatterers the refractive index has a

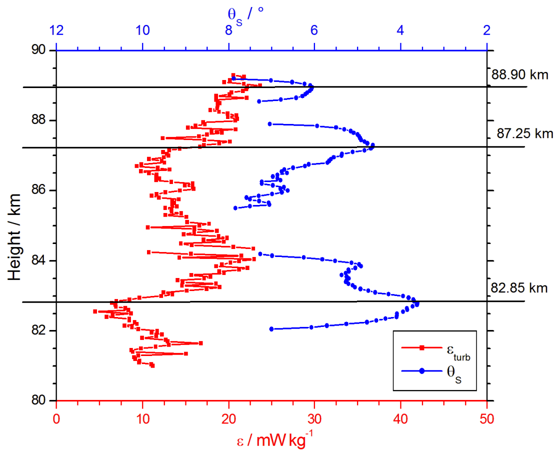

Figure 3. Turbulent energy dissipation rate ε determined from spectral width measurements (bottom axis) and the aspect sensitivity parameter (top axis) around the launch time. The horizontal lines mark the altitudes where the gradients in θ_s are zero.

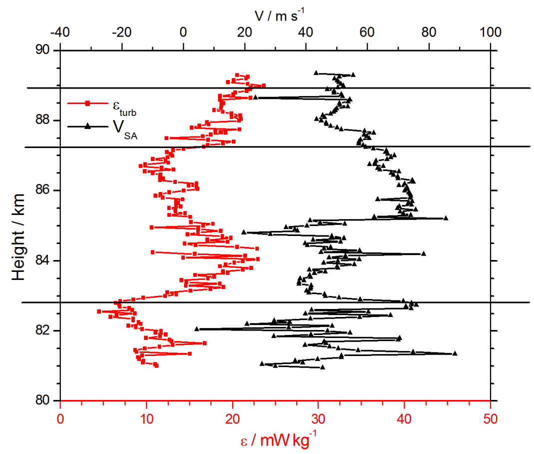

Figure 4. Height profile of the turbulent energy dissipation rate ε (bottom axis) and the simultaneously achieved horizontal wind field in beam direction towards NW (top axis).

form like $\exp\left(-(x^2+y^2)/l_x^2 + z^2/l_z^2\right)$ [16, 15]. With this background and the discussions in [17, 18] a ratio of the horizontal to vertical scales can be written as

$$\left(\frac{l_x}{l_z}\right)^2 = \left(\frac{\lambda^2/l_z^2}{8\pi^2 \sin^2\theta_s} + 1\right), \qquad (3)$$

where λ is the radar wavelength. The 1/e half-depth l_z of the eddy is in the range between 0.15λ and 0.32λ with a most likely value of $l_z \simeq 0.23\lambda$ [15].

3. RESULTS AND DISCUSSION

The case study documented here was carried out for the period when the ECOMA-04 rocket was launched on June 30th, 2008 at 13:22 UTC. During this rocket flight a double layered structure of PMSE was observed by the ALWIN radar. Fig. 1 shows the backscattered echo from the vertically pointing radar beam with two strong echoing layers at the top and the bottom of the PMSE. Tilting the radar beam towards north-west the top layer shows still a strong echo but the bottom layer nearly disappeared. Assuming that this variation is caused by the anisotropy of the scatterers and not by the horizontal inhomogeneities as supported by the concurrent rocket observations of [19]. This observation suggests a strong aspect sensitive layer at the bottom of the PMSE. Inbetween the layers of strong PMSE weaker echoes are observed, especially in the vertical beam.

For the further discussion a short period of ± 7.5 min around the rocket launch was selected and the average of this period was used to determine the parameters of interest. The height profiles of the signal strengths for the vertical and the 7° off-zenith pointing beams are shown in Fig. 1 (full lines) and it can be clearly seen that the signal of the lower layer is very weak in the tilted beam. The echoes of the top layer are stronger and the layer is seen in the vertical and the tilted beam. The aspect sensitivity parameter was calculated from Eq. 2 and shows a high aspect sensitivity between 82 and 83 km (low aspect angle). At the altitudes of the top PMSE layer the aspect sensitivity is lower compared to the bottom layer (larger θ_s). This observation suggest backscattering from more anisotropic turbulent structures from the bottom layer than from the top layer. Inbetween these two layers of strong backscatter weaker echoes are observed in both beams where the aspect angle could be estimated. Taking only the peak values of the aspect angles of the PMSE observed in this case the aspect sensitivity is decreasing with altitude and an estimate about the structures contributing to the backscatter can be derived.

The problem about the spatial extensions of the backscattering entities contributing to the radio wave scattering has been an open issue for many years, also because the discrimination between anisotropic turbulent structures and contributions from specular reflections are difficult to distinguish. A quantitative description was discussed in [20] and can be used to derive a limit to define the transition between anisotropic turbulence and specular reflections. As resumed from this discussion the turbulence strength estimated from spectral width measurements from the same radar returns was determined as discussed in [14]. Fig. 3 displays the turbulent energy dissipation rate estimated for the vertical pointing beam together with the observed aspect angle determined from the same spectra. The horizontal lines indicate the three altitudes where the aspect sensitivity has peaks.

The lowest layer at 82.95 km is characterized by a high aspect sensitivity indicating that the structures are more elongated in the horizonal direction. This altitude region is also characterized by a small value of the turbulence

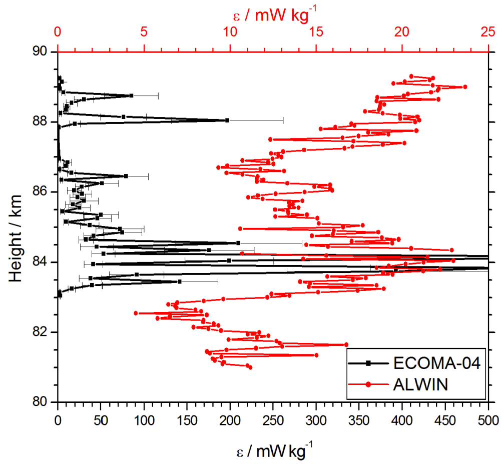

Figure 5. Turbulent energy dissipation rates ε determined from spectral width measurements using the radar (top axis) and from in-situ turbulence measurements obtained from the CONE instrument on the rocket (bottom axis). The scales are different for both instruments due to the different altitude and scale resolution.

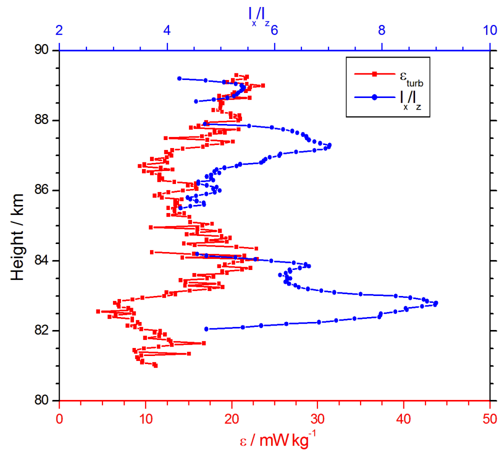

Figure 6. The aspect ratio l_x/l_z was determined from the aspect sensitivity parameter θ_s (top axis) and shows strong anisotropy in the lower part and less anisotropy for the top layer. The turbulent energy dissipation rate ε (bottom axis) represents the strength of turbulence observed simultanuously.

energy dissipation rate ε. The increase of the aspect sensitivity below this altitude is coupled to the decrease of turbulence strength from spectral width determination. The temperature observed in-situ by the CONE instrument decreases with altitude at the lower edge to a value below the frost point [19]. The simultaneously measured background wind field from the spaced-antenna experiment [21] is shown in Fig. 4 where the wind speed in north-west direction is about 76 m/s at the altitude of maximum aspect sensitivity. In the altitude of high wind speed the structures responsible for backscattering tending to be highly anisotropic. However, the aspect sensitive structures observed at this altitude are surely a mixure of anisotropic turbulent structures at several scales. Above 83 km a strong wind gradient evolves with increasing turbulence (Fig. 4). In this altitude range the aspect sensitivity decreases to a lower degree of anisotropic turbulence.

The increased turbulence was measured by the CONE instrument mounted on the ECOMA rocket (see [22] and references therein) which is shown in Fig. 5. During this flight the CONE instrument observed higher values of turbulence than the radar at altitudes around 84 km due to a different spatial resolution. In general, the height profiles show the same features, reduced turbulence between 86.5 and 87.5 km and extremly weak turbulence below 83 km. The radar measurements integrate over a volume of 10 $\times$ 0.3 km while the rocket-borne instrument measures the neutral and electron fluctuations in a very small volume and a very short time where the turbulence parameter is estimated from the inner scale in the turbulence spectrum [23]. For further comparison between radar and rocket measurements see [14].

In the altitude above the bottom layer with high aspect sensitivity strong turbulence dominates the radar backscatter and the aspect sensitivity decreases which is an indicator that the turbulent cells contributing to the scattering become less elongated in the horizontal dimension. Between 85 and 87 km the wind speed increases again and the turbulence dissipation rate decreases. The observation shows that the aspect sensitivity increases suggesting the structures become more elongated horizontally with increasing wind speed.

The altitude range around 89 km is characterized by strong radar backscatter and an aspect angle $\geq 6°$. There was active turbulence observed in the radar data and the in-situ CONE experiment. The in-situ rocket-borne measurements show thin layers of enhanced turbulence during the flight. The temporally and spatially averaged results from the radar soundings show similar features, especially the decrease of turbulence activity between the two layers. At this altitude the echo power was sufficiently strong that the effect could be compared with the in-situ measurements (Fig. 5).

Fig. 6 shows the l_x/l_z ratio calculated after Eq. 3 indicating that the echoes received from the bottom layer is strongly anisotrop with a horizontal-to-vertical ratio up to 9. This structure has a double peak which is clearly seen in this ratio. The peak around 84 km is at that height where the rocket-borne instrument has the two peaks of very strong turbulence (Fig. 5). Between these two turbulent layers the aspect sensitivity increases which indicates a more elongated and stratified zone of anisotropy.

Models were proposed to explain the formation of turbulent cells contributing to aspect sensitive backscatter [24, 25] where the refractive index is changed vertically across a turbulent layer. At the edges of the layer the eddies are elongated in the horizontal dimension. It is known also from numerical simulations [9, 10, 11]

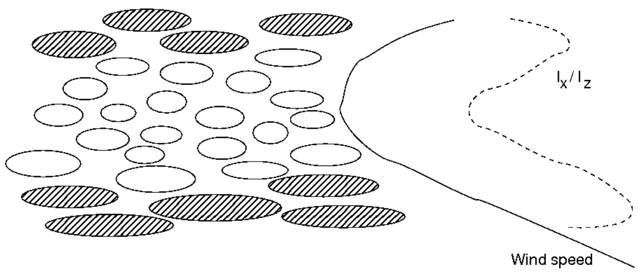

Figure 7. Schematic view of the anisotropic backscattering entities contributing to a a high aspect ratio l_x/l_z. In this example a gradient in the wind field creates an gradient in the refractive index and elongated scattering structures are responsible for the aspect sensitive backscatter.

that turbulent patches observed in stratified layers are highly anisotropic. The high aspect sensitivity arises from turbulence-induced irregularities with a vertical extension in the order of the Bragg scale (3 m) confined in layers with vertical extensions in the order of 30 – 300 m. Additionally, high acpect sensitive backscatter is confined to altitudes with strong gradients in the refractive index, generated by anisotropic turbulence at, especially, the boundaries separating the turbulent layer from the undisturbed surrounding.

Taking into account the anisotropy of turbulent patches at the boundaries of a turbulent layer and the formation of layered structures due to dynamically generated instabilities [26] the aspect sensitive backscatter in the particular example presented here can be discussed as a mixture of all these processes. Fig. 7 shows schematically how these layers contribute to the aspect ratio. It is specially drawn for a strong wind gradient but the idea is similar to [24, 25] and justified by modelling studies [9, 10, 11]. The lower PMSE layer is characterized by weak turbulence in the scales observed by the radar and the rocket-borne instrument in the lower part. The observation of a gradient in the wind speed suggest the formation of a dynamical instability similar to Kelvin-Helmholtz-Instabilities [26, 9] together with the existing ice particles creating inhomogeinities suitable for radar backscattering at the 3 m scale. Gradients formed in the boundary of stratified shear layers will produce strong anisotropic structures which result in highly aspect sensitive radar backscatter. The upper peak in the aspect sensitivity parameter is within a turbulent structure where the turbulence sensor observed two sharp layers of strong turbulent fluctuations separated by about 300 m. The height range between these turbulent layers contribute to an increased aspect sensitivity tending to specularity. Strong fluctuations in narrow layers produce gradients in the refractive index similar to the models in [24, 25].

The aspect sensitive radar echoes of the top layer of the PMSE combined with the turbulence measurements exhibits a similar explanation. The two turbulent layers observed in the in-situ experiment define the edges to the aspect sensitive layers. The stratified layer between these turbulent patches is characterized by reduced turbulence and decreasing aspect sensitivity. Interpreting this observation in terms of the anisotropy of turbulence induces irregularities contributing to the radar backscatter this fits exactly to the models mentioned above [25, 24, 26] with anisotropic turbulent eddies at the boundaries of a stratified isotrop turbulent layer. This finding is opposite to the explanation for the turbulent range of the upper part of the bottom layer where between the turbulent layers the backscattered radar echo shows a decreasing aspect sensitivity. The most important point is the change in the refractive index due to the existence of boundaries between scattering structures which were generated by enhanced turbulence.

4. SUMMARY

During the ECOMA campaign in 2008 an interesting radar observation shows multi-layered echoes in the vicinity of PMSE. The highly aspect sensitive echoes and the resulting fine structure in the aspect ratio can be explained with strong gradients in the turbulence activity. Therefore, the in-situ turbulence measurements by the CONE sensor during the ECOMA-04 flight show fine structures which could be correlated to the aspect sensitive layers and allow a detailed interpretation in the frame of the anisotropy of the backscattering entities. However, the radar observation is a temporal and spatial average of the dynamics of the atmosphere and the rocket-borne experiment only observes a snapshot of the dynamics. The combination of both methods is necessary to discuss the fine structure of the volume observed in this particular case.

ACKNOWLEDGMENTS

The authors thank the collegues from Andoya Rocketrange and ALOMAR Observatory for providing support in the operation of the radars and the members of the DLR Mobile Raketenbasis. Funding was provided by the European Research Council under the contract RITA-CT-2003-506208. The ECOMA project is supported by the German Space Center under DLR-grant 50 OE 0301 and the research council of Norway under grant 170848.

REFERENCES

[1] W. L. Ecklund and B. B. Balsley. Long-term observations of the arctic mesosphere with the MST radar at Poker Flat, Alaska. *J. Geophys. Res.*, 86(A9):7775–7780, 1981.

[2] J. Röttger, C. La Hoz, M.C. Kelley, U.-P. Hoppe, and C. Hall. The structure and dynamics of polar mesosphere summer echoes observed with the EISCAT 224 MHz radar. *Geophys. Res. Lett.*, 15(12):1353–1356, 1988.

[3] U.-P. Hoppe, C. Hall, and J. Röttger. First observations of summer polar mesospheric backscatter with a 224 MHz radar. *Geophys. Res. Lett.*, 15:28–31, 1988.

[4] M. Rapp and F.-J. Lübken. Polar mesosphere summer echoes (PMSE): Review of observations and current understanding. *Atmos. Chem. Phys.*, 4:2601–2633, 2004.

[5] R. Latteck, W. Singer, and H. Bardey. The Alwin MST radar - technical design and performances. In B. Kaldeich-Schürmann, editor, *Proc. 14th ESA Symp. on European Rocket and Ballon Programmes and related Research*, volume ESA SP-437, pages 179–184, 1999.

[6] M. Rapp and S. Robertson. Preface: ECOMA/MASS, aerosol particles near the polar summer mesopause. *Ann. Geophys.*, published online under http://www.ann-geophys.net/prefaces/preface219.pdf, 2009.

[7] J. Röttger and C.H. Liu. Partial reflection and scattering of VHF radar signals from the clear atmosphere. *Geophys. Res. Lett.*, 5(5):357–360, 1978.

[8] W. K. Hocking, R. Rüster, and P. Czechowsky. Absolute reflectivities and aspect sensitivities of VHF radio wave scatterers measured with the SOUSY radar. *J. Atmos. Terr. Phys.*, 48(2):131–144, 1986.

[9] J. Werne and D. C. Fritts. Anisotropy in a stratified shear layer. 26(4):263–268, 2001.

[10] U. Achatz. The primary nonlinear dynamics of modal and nonmodal perturbations of monochromatic inertia-gravity waves. *J. Atmos. Sci.*, 64(1):74–95, 2007.

[11] U. Achatz. Modal and nonmodal perturbations of monochromatic high-frequency gravity waves: Primary nonlinear dynamics. *J. Atmos. Sci.*, 64(6):1977–1994, 2007.

[12] W. K. Hocking. Strengths and limitations of MST radar measurments of middle-atmosphere winds. *Ann. Geophys.*, 15:1111–1122, 1997.

[13] W. K. Hocking, S. Fukao, T. Tsuda, M. Yamamoto, T. Sato, and S. Kato. Aspect sensitivity of stratospheric VHF radio wave scatterers, particularly above 15-km altitude. *Radio Sci.*, 25(4):613–627, 1990.

[14] N. Engler, R. Latteck, B. Strelnikov, W. Singer, and M. Rapp. Turbulent energy dissipation rates observed by Doppler MST Radar and by rocket-borne instruments during the MIDAS/MaCWAVE campaign 2002. *Ann. Geophys.*, 23(4):1147–1156, 2005.

[15] W. K. Hocking. Radar studies of small scale structure in the upper middle atmosphere and lower ionosphere. *Adv. Space Res.*, 7(10):327–338, 1987.

[16] B. H. Briggs and R. A. Vincent. Some theoretical considerations on remote probing of weakly scattering irregularities. *Aust. J. Phys.*, 26(6):805–814, 1973.

[17] D. Lesicar and W.K. Hocking. Studies of seasonal behaviour of the shape of mesosperic scatterers using a 1.98 MHz radar. *J. Atmos. Terr. Phys.*, 54(3/4):295–309, 1992.

[18] D. Lesicar, W.K. Hocking, and R.A. Vincent. Comparative studies of scatterers observed by MF radars in the southern hemisphere mesosphere. *J. Atmos. Terr. Phys.*, 56(5):581–591, 1994.

[19] B. Strelnikov, M. Rapp, I. Strelnikova, R. Latteck, N. Engler, T. A. Blix, and M. Hoppe, U.-P.and Friedrich. Small scale structures in neutral and plasma species in the middle atmosphere as observed during the ecoma rocket campaigns. In *Proceeding of the 19th ESA Symposium on European Rocket and Balloon Programmes and Related Research*, 2009.

[20] W. K. Hocking and A. M. Hamza. A quantitative measure of the degree of anisotropy of turbulence in terms of atmospheric parameters, with particular relevance to radar studies. *J. Atmos. Solar-Terr. Phys.*, 59(9):1011–1020, 1997.

[21] B. H. Briggs. The Analysis of Spaced Sensor Records by Correlation Techniques. In R.A. Vincent, editor, *Middle Atmosphere Program*, volume 13 of *Handbook for MAP*, pages 166–186. 1984.

[22] B. Strelnikov, M. Rapp, I. Strelnikova, N. Engler, and R. Latteck. Small-scale structures in neutrals and charged aerosol particles as observed during the ecoma/mass rocket campaign. *Ann. Geophys.*, 27(4):1449–1456, 2009.

[23] B. Strelnikov, M. Rapp, and F.-J. Lübken. A new technique for the analysis of neutral air density fluctuations measured in situ in the middle atmosphere. *Geophys. Res. Lett.*, 30(20), 2003.

[24] Ronald F. Woodman and Yen-Hsyang Chu. Aspect sensitivity measurements of VHF backscatter made with the Chung-Li radar: Plausible mechanisms. *Radio Sci.*, 24(2):113–125, 1989.

[25] W. K. Hocking. *Middle atmosphere program*, volume 30, chapter Target parameter estimation, pages 228–268. Handbook for MAP, 1989.

[26] Iain M. Reid. Radar observtions of stratified layers in the mesosphere and lower thermosphere (50-100 km). *Adv. Space Res.*, 10(10):7–19, 1990.